Published in "European Journal of Neuroscience 31(2): 273-285, 2010"
which should be cited to refer to this work.

Quantitative analysis of postnatal neurogenesis and neuron number in the macaque monkey dentate gyrus

Adeline Jabès,[1] Pamela Banta Lavenex,[1] David G. Amaral[2] and Pierre Lavenex[1]
[1]Laboratory of Brain and Cognitive Development, Department of Medicine, Unit of Physiology, University of Fribourg, Switzerland
[2]Department of Psychiatry and Behavioral Sciences, Center for Neuroscience, California National Primate Research Center, The M.I.N.D. Institute, UC Davis, USA

Keywords: development, hippocampus, infantile amnesia, memory, neurodevelopmental disorder, stereology

Abstract

The dentate gyrus is one of only two regions of the mammalian brain where substantial neurogenesis occurs postnatally. However, detailed quantitative information about the postnatal structural maturation of the primate dentate gyrus is meager. We performed design-based, stereological studies of neuron number and size, and volume of the dentate gyrus layers in rhesus macaque monkeys (*Macaca mulatta*) of different postnatal ages. We found that about 40% of the total number of granule cells observed in mature 5–10-year-old macaque monkeys are added to the granule cell layer postnatally; 25% of these neurons are added within the first three postnatal months. Accordingly, cell proliferation and neurogenesis within the dentate gyrus peak within the first 3 months after birth and remain at an intermediate level between 3 months and at least 1 year of age. Although granule cell bodies undergo their largest increase in size during the first year of life, cell size and the volume of the three layers of the dentate gyrus (i.e. the molecular, granule cell and polymorphic layers) continue to increase beyond 1 year of age. Moreover, the different layers of the dentate gyrus exhibit distinct volumetric changes during postnatal development. Finally, we observe significant levels of cell proliferation, neurogenesis and cell death in the context of an overall stable number of granule cells in mature 5–10-year-old monkeys. These data identify an extended developmental period during which neurogenesis might be modulated to significantly impact the structure and function of the dentate gyrus in adulthood.

Introduction

The dentate gyrus is one of only two regions of the mammalian brain (the olfactory bulb being the other) where substantial neurogenesis has been unequivocally shown to occur postnatally (Altman & Das, 1965; Rakic & Nowakowski, 1981; Cameron *et al.*, 1993). In primates, although the majority of the neurons in the hippocampal formation are generated prenatally (Nowakowski & Rakic, 1981; Eckenhoff & Rakic, 1988; Arnold & Trojanowski, 1996), neurogenesis has been shown to continue throughout life in the dentate gyrus of marmosets (Gould *et al.*, 1998), macaque monkeys (Gould *et al.*, 1999b; Kornack & Rakic, 1999) and humans (Eriksson *et al.*, 1998). However, and despite the interest and importance of understanding the regulation of neurogenesis across the lifespan (Gould & Gross, 2002; Kempermann, 2002; Nottebohm, 2002), there is no detailed quantitative information regarding postnatal neurogenesis in the primate dentate gyrus.

Early studies of neurogenesis using the radioactive thymidine-labeling technique in macaque monkeys reported a sharp decrease in neuron production within 3–4 months after birth, but failed to demonstrate neurogenesis in adult individuals (Rakic & Nowakowski, 1981; Rakic, 1985; Eckenhoff & Rakic, 1988). Later studies using the cell division marker 5′-bromo-2-deoxyuridine (BrdU) revealed that neurogenesis occurs in adult primates (Eriksson *et al.*, 1998; Gould *et al.*, 1999b; Kornack & Rakic, 1999), but did not fully appreciate its importance with respect to the addition of new neurons and their maturation into hippocampal circuits. Furthermore, only limited descriptions of the number of neurons observed at birth as compared with that observed in adult primates have ever been published (Seress, 1988, 1992; Lavenex *et al.*, 2007a). All the available data, therefore, derive from miscellaneous studies using different methodologies in different species at various developmental stages. Notably absent is a systematic, quantitative evaluation of the postnatal structural development of the primate dentate gyrus.

Quantitative information regarding the normal development and structural organization of the brain is necessary to generate useful models of normal and abnormal brain functions (Banta Lavenex *et al.*, 2001; Altemus *et al.*, 2005). For example, 'enriched' environments were shown to regulate neurogenesis in developing, 21-day-old mice, leading to changes in neuron number and hippocampal function (Kempermann *et al.*, 1997). When such manipulations are imposed on 6- or 18-month-old mice, neurogenesis is also regulated but neither structural nor functional effects are observed (Kempermann *et al.*, 1998). Such results indicate that certain environmental factors, either beneficial or pathogenic, might impact hippocampal structure and function during specific periods of development. Because the primate

Correspondence: Dr P. Lavenex, as above.
E-mail: pierre.lavenex@unifr.ch

dentate gyrus undergoes substantial postnatal maturation (Giedd *et al.*, 1996; Saitoh *et al.*, 2001; Lavenex *et al.*, 2007a) and because developmental abnormalities of the dentate gyrus are thought to contribute to the etiology of neurological disorders such as autism (Courchesne, 2002), schizophrenia (Harrison, 1999) and epilepsy (Sloviter, 1994), it is of particular importance to establish the developmental trajectory during which intrinsic or extrinsic factors might impact specific aspects of its structural and functional maturation.

In this study, we used stereological techniques to characterize and quantify the morphological changes underlying the structural maturation of the macaque monkey dentate gyrus during early postnatal development.

Materials and methods

Animals

Twenty-four rhesus monkeys, *Macaca mulatta*; four 1-day-olds (2 M, 2 F), four 3-month-olds (2 M, 2 F), four 6-month-olds (2 M, 2 F), four 9-month-olds (2 M, 2 F), four 1-year-olds (2 M, 2 F) and four adults [5.3, 9.4 (M), 7.7 and 9.3 (F) years old] were used for this study. Monkeys were born from multiparous mothers and raised at the California National Primate Research Center (CNPRC). They were maternally reared in 2000-m^2 outdoor enclosures and lived in large social groups until they were killed. All experimental procedures were approved by the Institutional Animal Care and Use Committee of the University of California, Davis, and were in accordance with the National Institutes of Health guidelines for the use of animals in research.

Each monkey was injected with the cell-division marker, BrdU (150 mg/kg i.p.; Boehringer Mannheim) 4 weeks prior to death. For the four animals collected at birth, we injected the mothers with the same concentration of BrdU 4 weeks prior to expected delivery (actual intervals, 24, 29, 31, 35 days). The dose of BrdU was selected in order to maximize the amount of labeling that is detectable, while minimizing the possible toxic side-effects of the marker observed during development (Kolb *et al.*, 1999; Cameron & McKay, 2001). The interval of 4 weeks between BrdU injection and death was chosen to allow sufficient time for cell differentiation, migration and possible integration into the hippocampal circuitry (Gould *et al.*, 1999a; Kornack & Rakic, 1999). Monkeys were deeply anesthetized with an intravenous injection of sodium pentobarbital (50 mg/kg i.v.; Fatal-Plus, Vortech Pharmaceuticals, Dearborn, MI, USA) and perfused transcardially with 1% and then 4% paraformaldehyde in 0.1 M phosphate buffer (PB; pH 7.4) following protocols previously described (Banta Lavenex *et al.*, 2006; Lavenex *et al.*, 2009a).

Coronal sections were cut using a freezing microtome in six 30-μm series and one series at 60 μm (Microm HM 450; Microm International, Germany). The 60-μm sections were collected in 10% formaldehyde solution in 0.1 M PB (pH 7.4) and postfixed at 4°C for 4 weeks prior to Nissl staining with thionin. All other series were collected in tissue collection solution (TCS) and kept at −70°C until further processing (Lavenex *et al.*, 2009a).

Nissl staining with thionin

The procedure for Nissl-stained sections followed our standard laboratory protocol described previously (Lavenex *et al.*, 2009a).

Ki-67 immunohistochemistry

We processed one series of 30-μm-thick sections (960 μm apart) for the immunohistochemical detection of the endogenous protein Ki-67, to study cell proliferation. Sections were taken from TCS and rinsed for 4 × 10 min in 0.02 M KPBS (pH 7.4), incubated for 20 min in 0.3% H_2O_2 in 100% methanol at 4°C, rinsed for 3 × 10 min in 0.02 M KPBS and incubated for 1 h in a blocking solution comprised of 0.5% Triton X-100 (TX-100; Fluka, Cat. no. 93418), 5% normal goat serum (NGS; Chemicon, Cat. no. CHMCS26-LITER) in 0.02 M KPBS at room temperature. Sections were then incubated for 48 h in primary antiserum (rabbit anti-Ki-67; Zymed Laboratories, Cat. no. 18-0191, at 1 : 500 in 0.3% TX-100, 2% NGS, 0.02 M KPBS) at 4°C, rinsed for 3 × 10 min at room temperature in 0.02 M KPBS containing 2% NGS, incubated for 1 h in secondary antiserum (biotinylated goat anti-rabbit IgG; Vector Laboratories, Cat. no. BA-1000, at 1 : 227 in 0.3% TX-100, 2% NGS, 0.02 M KPBS), rinsed for 3 × 10 min in 0.02 M KPBS containing 2% NGS, incubated for 1 h in avidin-biotin complex (Biomeda, Cat. no. 11-001-JEFF1) at room temperature, rinsed for 3 × 10 min in 0.02 M KPBS containing 2% NGS, incubated for another 45 min in secondary antiserum, rinsed for 3 × 10 min in 0.02 M KPBS, incubated for another 30 min in avidin-biotin complex, rinsed for 3 × 10 min in 0.1 M Tris buffer and incubated for 30 min in a 0.05% diaminobenzidine (DAB; Sigma-Aldrich Chemicals, St Louis, MO, USA, Cat. no. D9015-100MG)/0.04% H_2O_2 solution. The sections were then rinsed, mounted onto gelatin-coated slides, defatted and coverslipped with DPX (BDH Laboratories, Poole, UK). Following the plotting of Ki-67-labeled cells with StereoInvestigator 7.0 (see below), sections were counterstained for Nissl with thionin: slides were placed in 100% xylene until the coverslips could be removed, kept overnight in xylene and rehydrated though a series of ethanols (2 × 2 min in 100%, 2 min in 95%, 2 min in 70%, 2 min in 50%), dipped in two separate baths of dH_2O, and stained for 5 s in a 0.25% thionin solution (Fluka, Cat. no. 72048). Sections were then dipped in two separate baths of dH_2O, 4 min in 50% ethanol, 4 min in 70% ethanol, 2 min in 95% ethanol + glacial acid (1 drop per 100 mL of ethanol), 4 min in 95% ethanol, 2 × 4 min in 100% ethanol, 3 × 4 min in xylene, and coverslipped with DPX (BDH Laboratories).

BrdU and cell-specific marker immunohistochemistry

We used the exogenous cell-division marker, BrdU, in combination with the neuron-specific marker, NeuN, and glia-specific marker, S100beta, to study the fate of newly generated cells during development. The portion of the coronal brain section containing the hippocampal formation was dissected for free-floating processing. Sections were first rinsed 3 × 5 min in 0.1 M phosphate-buffered saline (PBS, pH 7.4), incubated for 1 h in 2 N HCl at room temperature, followed by 15 min in 0.1 M borate buffer (pH 8.5) and rinsed 2 × 5 min in 0.1 M PBS (pH 7.4). They were then incubated for 1 h in blocking serum [PBS + 0.3% TX-100 + 5% normal donkey serum (NDS; Biomeda, Cat. no. ES1031)] and for 72 h in a primary antiserum cocktail [1 : 1000 sheep anti-BrdU (Fitzgerald, Cat. no. 20-BS17) + 1 : 1000 mouse anti-NeuN (Chemicon, MAB 377) + 1 : 1000 rabbit anti-S100beta (Swant, Cat. no. 37A) in 0.1 M PBS + 0.3% TX-100 + 2% NDS] at 4°C with gentle agitation on a rotating platform. Sections were then rinsed 3 × 5 min in 0.1 M PBS and incubated for 4 h at room temperature in a secondary antiserum cocktail [1 : 1000 Cy2-conjugated anti-sheep IgG (Jackson Laboratories, 713-225-147) + 1 : 1000 Cy3-conjugated anti-mouse IgG (Jackson Laboratories, 715-165-150) + 1 : 1000 Cy5-conjugated anti-rabbit IgG (Jackson Laboratories, 711-175-152) in 0.1 M PBS + 0.3% TX-100 + 2% NDS] with gentle agitation on a rotating platform. From this point on, sections were always protected from light.

Sections were then rinsed 3 × 5 min in 0.1 M PBS mounted on gelatin-coated slides and air-dried for 5 days at room temperature. Sections were then dehydrated through a graded series of ethanol solutions and coverslipped with DPX (BDH Laboratories).

Terminal deoxynucleotidyl transferase-mediated dUTP-biotin nick-end labeling (TUNEL) staining

We used the TUNEL method to evaluate cell death. The TUNEL method is a well-established staining technique used to detect DNA fragmentation that occurs in dying cells (Gavrieli *et al.*, 1992; Biebl *et al.*, 2000; Oppenheim *et al.*, 2001; Amrein *et al.*, 2004). Processing was performed using the *In Situ* Cell Death Detection Kit, POD (Roche Diagnostics GmbH, Germany). The portion of the coronal brain section containing the hippocampal formation was dissected for processing. Sections were rinsed three times in filtered 0.05 M PB (pH 7.4), mounted on Super Frost^{+} slides (Thermo Scientific, Menzel GmbH, Cat. no. 85-0911-00) and air-dried for 7 days at room temperature. Slides were then rinsed 2 × 5 min in dH_2O and incubated for 20 min in 100% methanol containing 0.3% H_2O_2 at room temperature. Slides were then rinsed 3 × 2 min in 0.1 M PBS (pH 7.4), incubated for 20 min in 50 mM Tris-HCl (pH 8.0), containing 10 mM $CaCl_2$ and 20 μg/mL proteinase K (Promega, Cat. no. V302B) at room temperature, and rinsed 3 × 5 min in 0.1 M PBS (pH 7.4). Slides were then carefully dried around the sections, covered with 50 μL of the TUNEL reaction mixture (Roche Diagnostics GmbH, Germany, Cat. no. 11684817910) and a glass coverslip, and then incubated for 1 h at 37°C. Slides were rinsed with dH_2O to remove the coverslip and rinsed 3 × 2 min in 0.1 M PBS (pH 7.4). Slides were again carefully dried around the sections, covered with 50 μL of Converter-POD and a glass coverslip, and incubated for 30 min at 37°C. Slides were rinsed 2 × 5 min in 0.1 M PBS (pH 7.4), 1 × 5 min in 50 mM Tris (pH 7.4) and incubated in a 0.05% DAB (Sigma-Aldrich Chemicals; Cat. no. D9015-100MG/ 0.04% H_2O_2) for 15 min at room temperature. Slides were then rinsed 2 × 5 min in 50 mM Tris (pH 7.4), dipped once in dH_2O and air-dried overnight at 37°C. Sections were then dehydrated through a graded series of ethanol solutions and coverslipped with DPX (BDH Laboratories). Following the plotting of TUNEL-labeled cells with StereoInvestigator 7.0 (see below), sections were counterstained for Nissl as described previously for sections processed for Ki-67 immunochemistry.

Data analysis

Anatomical boundaries of the dentate gyrus

The cytoarchitectonic organization of the dentate gyrus has been described previously (Lavenex & Amaral, 2000; Amaral & Lavenex, 2007; Amaral *et al.*, 2007; Lavenex *et al.*, 2009a). We delineated the three layers of the dentate gyrus (i.e. the molecular, granule cell and polymorphic layers) according to these descriptions for all subsequent analyses. However, although it is generally considered that new neurons are generated in the subgranular zone just beneath the granule cell layer in rodents (but see Namba *et al.*, 2005), the exact extent of the subgranular zone is neither clearly described nor identifiable in monkeys (Eckenhoff & Rakic, 1984; Seress, 1992; Amaral *et al.*, 2007). As compared with the rodent, the primate polymorphic layer has thinned to a very narrow subgranular region (see Fig. 2D of Amaral *et al.*, 2007). The proliferative zone therefore seems to encompass the polymorphic layer and the deep portion of the granule cell layer, and its extent appears to vary throughout postnatal development (Seress, 1992). Indeed, we also observed Ki-67-labeled and BrdU/NeuN-positive cells throughout the polymorphic layer and in the granule cell layer. We therefore combined the data for the polymorphic and granule cell layers for the analyses of cell proliferation, neurogenesis and cell death (see below).

Neuron counts and volume measurements

Neuron counts and volume measurements were performed with StereoInvestigator 7.0 (Microbrightfield, Williston, VT, USA). The volume of the three layers of the dentate gyrus were measured according to the Cavalieri principle on the Nissl-stained sections cut at 60 μm (Gundersen & Jensen, 1987; West & Gundersen, 1990; Lavenex *et al.*, 2000a,b). About thirty sections per animal (480 μm apart), with the first section selected randomly within the first two sections through the dentate gyrus, were used for the measurements of the volumes of the molecular, granule cell and polymorphic layers.

The total number of neurons in the granule cell layer was determined using the optical fractionator method (West *et al.*, 1991; Lavenex *et al.*, 2000a,b). This design-based method enables the estimation of the number of neurons that is independent of volume estimates (Lavenex *et al.*, 2000b; Pravosudov *et al.*, 2002). About thirty sections per animal (480 μm apart), with the first section selected randomly within the first two sections through the granule cell layer, were used for the neuron counts. We used a 100× Plan Fluor oil objective (N.A. 1.30) on a Nikon Eclipse 80i microscope (Nikon Instruments, Melville, NY, USA) linked to PC-based StereoInvestigator 7.0. The sampling scheme was as follows: average section thickness: 11.51 μm (range 8.50–14.53); scan grid: 300 × 300 μm (with random orientation); counting frame: 15 × 15 μm; dissector height: 5 μm; and guard zones: 2 μm. Section thickness was measured at every other counting site. This sampling scheme was established to obtain individual estimates of neuron number with coefficients of error (CE) lower than 0.10.

The volume of granule cell somas was determined using the Nucleator method on the Nissl-stained sections (Gundersen, 1988; Lavenex, 2009; Lavenex *et al.*, 2009a). Between 200 and 400 neurons, every fourth counting site chosen randomly during the optical fractionator analysis (i.e. neuron counts), were measured.

Ki-67-labeled cell counts

Because of the low number of labeled cells in adult animals, we did not use a stereological probe to count the number of Ki-67-labeled cells. The total number of Ki-67-positive cells was determined by plotting exhaustively all labeled cells throughout the dentate gyrus with the StereoInvestigator analysis system and a 40× Plan Fluor objective (N.A. 0.75). Sections were then counterstained for Nissl in order to define the borders of the different layers of the dentate gyrus. This method, which does not take into account the problems of oversampling and lost caps, does not affect the conclusion drawn from our study, as all samples were treated identically. About six sections per animal [1 in 64 sections (1920 μm apart)], with the first section selected randomly within the first two sections through the granule cell layer, were used. The number of Ki-67-positive cells counted in the sampled sections was multiplied by the inverse of the section sampling fraction (ssf = 1/64 sections) to obtain estimates of the total number of proliferative cells in the dentate gyrus. We present the number of Ki-67-positive cells in the molecular layer and in the combined granule cell and polymorphic layers (see Anatomical boundaries of the dentate gyrus).

BrdU-labeled cell counts

BrdU-positive cells were analysed in a two-step process. First, all BrdU-labeled cells within the dentate gyrus were plotted with the StereoInvestigator analysis system in every section processed for BrdU immunochemistry. Ten–15 sections per animal [one in four sections of a 30-μm series (960 μm apart)], with the first section selected randomly within the first two sections through the granule cell layer, were used to estimate the number of BrdU-labeled cells in the granule cell layer. Because of the low number of labeled cells in adult individuals, we did not use a stereological probe to count the number of BrdU-labeled cells. Direct counting was performed with a Nikon Eclipse 80i microscope with a D-FL Epi-fluorescence attachment (X-Cite 120 fluorescence illumination system; FITC filter) and a 40 × Plan Fluor objective (N.A. 0.75). Therefore, all labeled cells were counted through the entire thickness of the section. This method, which does not take into account the problems of oversampling and lost caps, does not affect the conclusions drawn from our study, as all samples were treated identically. The number of BrdU-labeled cells counted in the sampled sections was multiplied by the inverse of the section sampling fraction to obtain estimates of the total number of BrdU-labeled cells in each layer.

Second, the phenotype of BrdU-labeled cells was determined based on the co-localization of BrdU and NeuN (for neurons), or BrdU and S100beta (for astrocytes) with a confocal microscope (DM6000, Leica Microsystems, Wetzlar, Germany). We used a 63× glycerol objective (HCX PlanApo, N.A. 1.30) and a digital magnification of 3×. We performed a sequential acquisition to avoid 'cross-talk' between different excitation lasers and photomultiplier detection systems. The settings were as follows: for the visualization of BrdU (fluorophore Cy2): excitation: 488 nm (argon laser); detection: FITC filter, wavelength 490–540, gain 1083, offset -38.1, pinhole 51.46 μm. For the visualization of NeuN (fluorophore Cy3): excitation: 561 nm (DPSS laser); detection: TRITC filter, wavelength 590–630, gain 1030, offset 1.9, pinhole 75 μm. For the visualization of S100beta (fluorophore Cy5): excitation: 633 nm (HeNe laser); detection: Cy5 filter, wavelength 640–710, gain 830, offset -15.2, pinhole 102.87 μm. For each acquisition, we used a frame average of 30 at a speed of 8000 Hz and z-steps of 1 μm. We analysed 5–15 sections per animal, depending on the total number of BrdU-labeled cells plotted and counted in the first stage of the analysis (see above). In cases with fewer than 50 BrdU-labeled cells plotted throughout the dentate gyrus, every labeled cell was analysed. In cases with 50–1000 BrdU-labeled cells, the sampling scheme was adjusted so that an average of 68 labeled cells were analysed. In cases with more than 1000 BrdU-labeled cells, an average of 113 cells were analysed. The percentage of sampled BrdU-labeled cells expressing NeuN, S100beta or neither in each layer was multiplied by the total number of BrdU-labeled cells per layer to obtain the total number of cells of each phenotype per layer. We present the number of BrdU/NeuN-positive, BrdU/S100-beta-positive, BrdU/none-positive cells in the molecular layer and in the combined granule cell and polymorphic layers (see Anatomical boundaries of the dentate gyrus).

TUNEL-labeled cell counts

The number of TUNEL-positive cells was determined as described for the Ki-67 analysis. Sections were then counterstained with Nissl in order to define the borders of the different layers of the dentate gyrus. The number of TUNEL-positive cells per layer counted in the sampled sections was multiplied by the inverse of the section sampling fraction (ssf = 1/32 sections) to obtain the total number of TUNEL-labeled cells per layer. We present estimates of the number of TUNEL-positive cells in the molecular layer and in the combined granule cell and polymorphic layers (see Anatomical boundaries of the dentate gyrus).

Statistics

We performed analyses of variance (ANOVAs) with age as a factor on volume and total neuron numbers, as these data were normally distributed. *Post hoc* analyses were performed with the Fisher-PLSD test. We performed non-parametric Kruskal–Wallis analyses for data on cell proliferation, neurogenesis and cell death, as these data were not distributed normally. *Post hoc* analyses were performed with the Student's–Newman–Keuls test. Significance level was set at $P < 0.05$ for all analyses. No gender effect was found for any of the measured parameters, so that data from both genders were combined for presentation. We also evaluated both left and right dentate gyrus in a systematic manner: we measured the left dentate gyrus for one male and one female, and the right dentate gyrus for one male and one female, in each age group. No lateralization effect was found for any of the measured parameters. All sections used in this study were coded to allow blind analysis, and the code was broken only after completion of the analyses.

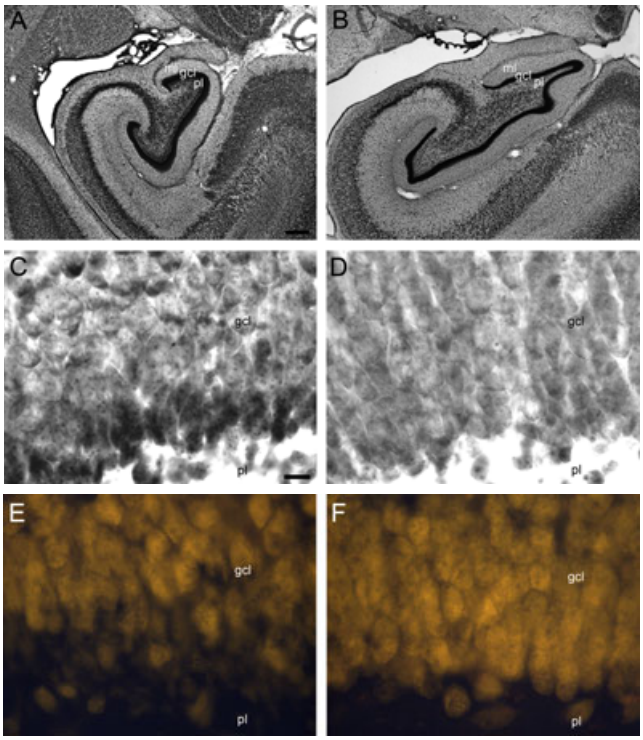

FIG. 1. Coronal Nissl-stained sections at mid-rostrocaudal level through the dentate gyrus of a newborn (A) and 7.7-year-old (B) macaque monkey (*Macaca mulatta*). gcl, granule cell layer; ml, molecular layer; pl, polymorphic layer. Scale bar: 500 μm (A, applies to A and B). (C) Nissl-stained section illustrating the presence of a large population of immature neurons in the deep portion of the granule cell layer of a newborn monkey. (D) Nissl-stained sections showing the same area in an adult monkey. Note the absence of the large population of immature neurons in the adult as compared with the newborn monkey. (E) NeuN-immunostained section showing that the large population of cells identified as immature granule cells in Nissl preparations (C) are consistently but faintly labeled with NeuN. (F) NeuN-immunostained section showing the same area in an adult monkey. All neurons in the adult granule cell layer are heavily labeled with NeuN. Scale bar: 10 μm (C, applies to C–F).

Results

Even a cursory examination of the neonatal and adult macaque monkey dentate gyrus is sufficient to demonstrate that the primate dentate gyrus is far from mature at birth (Fig. 1). In the following sections, we provide detailed information on cell proliferation (Ki-67 immunohistochemistry), neurogenesis (BrdU/NeuN or S100beta immunohistochemistry), cell death (TUNEL method), total neuron number, neuronal soma size and neuropil volume (Nissl-stained sections) in the dentate gyrus of developing monkeys from birth to 1 year of age, and in mature monkeys between 5 and 10 years of age.

Ki-67 immunohistochemistry

Cell proliferation was measured via immunohistochemical detection of the endogenous marker of cell division, protein Ki-67. The number of Ki-67-positive cells differed between age groups in the combined granule cell and polymorphic layers (Fig. 2; $H = 17.950$, $P = 0.003$). There was a substantial number of Ki-67-labeled cells throughout the granule cell and polymorphic layers of newborn monkeys (107888 ± 17331). At 3 months old, the number of Ki-67-positive cells decreased to about 55% of the level observed at birth (59824 ± 10729; $P < 0.05$). The level of cell proliferation remained relatively stable between 6 months and 1 year old, with an average of 31 872 ± 3558 labeled cells, corresponding to about 30% of the newborn level. The number of Ki-67-labeled cells found in 5–10-year-old monkeys was about 3% of the level observed at birth (3520 ± 1068; $P < 0.05$).

The number of Ki-67-positive cells differed between age groups in the molecular layer (Fig. 2; $H = 15.670$, $P = 0.008$), but its developmental profile differed slightly from that observed in the granule cell and polymorphic layers. The number of Ki-67-labeled cells was 40224 ± 7916 in newborn monkeys, and decreased to about 34% of the newborn level at 3 months of age (13504 ± 3282; $P < 0.05$). Although we could not demonstrate a significant difference between age groups after 3 months of age (we found an average of 10276 ± 1642 labeled cells in the molecular layer of monkeys between 3 months and 1 year of age, about 25% of the newborn level), the number of Ki-67-labeled cells found in 5–10-year-old monkeys was only about 8% of the level observed at birth (3104 ± 692; $P < 0.05$).

These data reveal a very high level of cell proliferation in the monkey dentate gyrus at birth, followed by an intermediate level persisting throughout the first year of life. Although cell proliferation clearly persists beyond 1 year of age, its level across all layers of the dentate gyrus of 5–10-year-old monkeys is close to 5% of the level observed in newborn monkeys.

BrdU/NeuN/S100beta immunohistochemistry

Differentiation and survival of proliferating cells was examined 4 weeks after the injection of the exogenous cell-division marker BrdU. The number of BrdU-positive cells expressing the neuron-specific marker NeuN differed significantly between age groups in the combined granule cell and polymorphic layers (Fig. 3A; $H = 19.639$, $P = 0.001$). It decreased between birth (20 389 ± 1704) and 3 months of age (14932 ± 1623; $P < 0.05$; 73% of the newborn level), and between 3 and 6 months of age ($P < 0.05$). From 6 months to 1 year of age, the number of BrdU/NeuN-positive cells remained at an intermediate level (average: 4186 ± 751; 21% of the newborn level), and finally reached 0.7% of newborn level at 5–10 years of age (136 ± 46). The number of BrdU-positive cells expressing S100beta in the combined granule cell and polymorphic layers showed a similar developmental profile (Fig. 3A; $H = 20.100$, $P = 0.001$). It decreased between birth (40 018 ± 6550) and 3 months of age (9058 ± 780; $P < 0.05$; 23% of the newborn level), and between 3 and 6 months of age ($P < 0.05$). From 6 months to 1 year of age the number of BrdU/S100beta-positive cells remained at an intermediate level (average: 3117 ± 695; 8% of the newborn level), and finally reached 0.9% of the newborn level at 5–10 years of age (376 ± 150; see also Table S1).

The number of BrdU/S100beta-labeled cells in the molecular layer differed between age groups (Fig. 3C; $H = 18.876$, $P = 0.002$). BrdU-positive cells expressing NeuN were never observed in the molecular layer, but not all BrdU-labeled cells were found to express S100beta (Table S2). The number of BrdU-labeled cells co-expressing S100beta decreased from birth (21909 ± 2956) to 3 months of age (3547 ± 492; $P < 0.05$; 16% of birth level). The number of BrdU/S100beta-positive cells remained at an intermediate level between 6 months and 1 year of age (average 1111 ± 109; 5% of newborn level), and

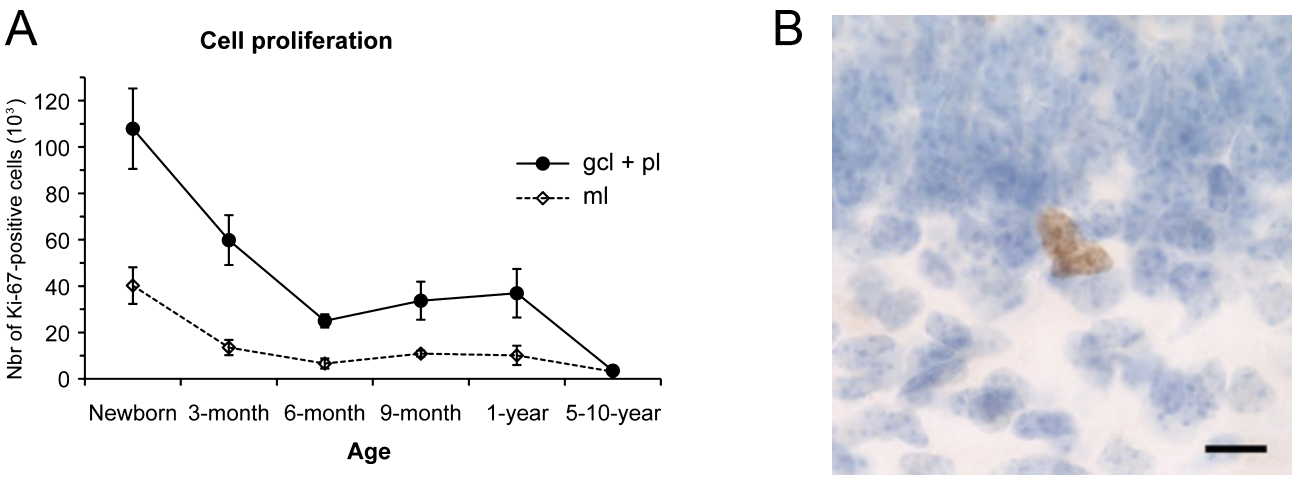

FIG. 2. Ki-67-immunohistochemistry. (A) Number of Ki-67-positive cells in the molecular layer (white diamonds) and in the combined granule cell and polymorphic layers (black circles) of the macaque monkey dentate gyrus through early postnatal development and in adulthood. Note the intermediate level of cell proliferation between 3 months and 1 year of age. (B) Photomicrograph of Ki-67-labeled cells in the granule cell and polymorphic layers of the dentate gyrus. Scale bar: 10 μm. Abbreviations, see Fig. 1.

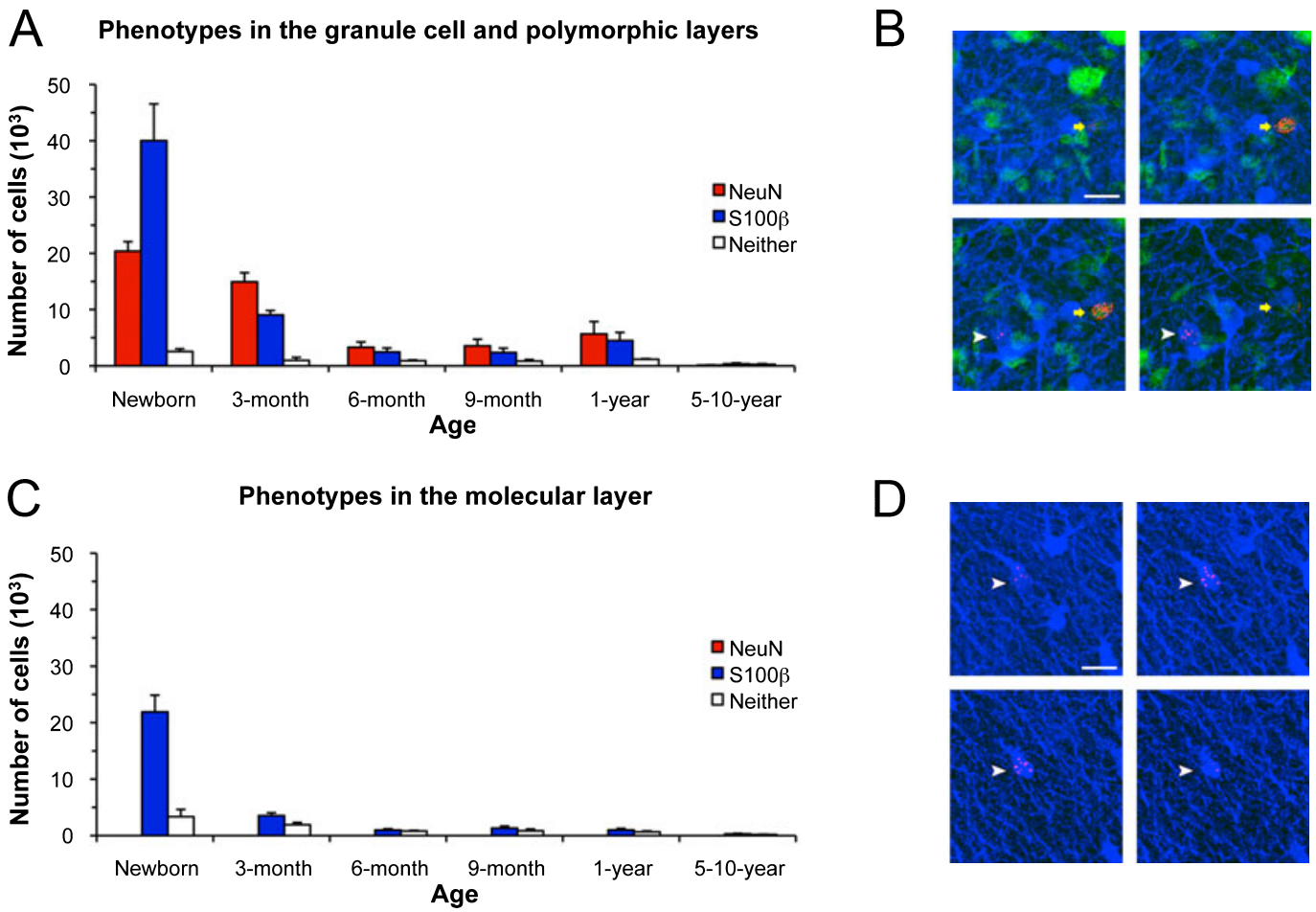

FIG. 3. Phenotypes of BrdU-labeled cells in the macaque monkey dentate gyrus, 4 weeks following BrdU injection (150 mg/kg). (A) Phenotypes of BrdU-labeled cells in the combined granule cell and polymorphic layers. Note the significant rate of BrdU/NeuN-positive cells until 1 year old. (B) Confocal image of BrdU/NeuN-positive (yellow arrow) and BrdU/S100beta-positive (white arrowheads) cells at the border between the granule cell and polymorphic layers. Scale bar: 10 μm (applies to all panels). (C) Phenotypes of BrdU-labeled cells in the molecular layer. Note the absence of BrdU/NeuN-positive cells in the molecular layer. (D) Confocal image of a BrdU/S100beta-positive cell (white arrowhead) in the molecular layer. The different panels in (B) and (D) represent different planes of section (1 μm apart) through the depth of the labeled cells. Scale bar: 10 μm (applies to all panels).

decreased to 1% of newborn level at 5–10 years of age (300 ± 85). These data confirm that no new neurons are incorporated into the molecular layer of the dentate gyrus during the monkey's early postnatal or adult life.

Interestingly, the overall distribution of BrdU-labeled cells differed from that of Ki-67-labeled cells across the polymorphic and granule cell layers (Fig. 4A–F). Indeed, about 86% of Ki-67-labeled cells were clearly located in the polymorphic layer across all age groups, whereas only 66% of BrdU-positive cells, marked by a single BrdU injection (150 mg/kg, i.p.) 4 weeks prior to brain collection, were located in the polymorphic layer (data not shown). Considering specifically the number of BrdU/NeuN-positive cells, 43% were clearly located in the granule cell layer in newborn monkeys, 24% in monkeys between 3 months and 1 year of age, and 88% in 5–10-year-old monkeys. These findings indicate that only a portion of newly generated neurons have migrated into the granule cell layer 1 month after cell division, and they typically remained in the deeper portion of the layer (closer to the polymorphic layer) at that stage.

We also calculated the number of newly-generated neurons that could potentially be integrated into the granule cell layer of 5–10-year-old monkeys per day. We found an average of 114 BrdU/NeuN-positive cells unambiguously located in the granule cell layer 4 weeks following BrdU injection. We considered that BrdU can label dividing cells for up to 2 h following a single injection (Cameron & McKay, 2001), and assumed a cell cycle of about 25 h similar to that observed in mature rodents (Cameron & McKay, 2001; Hayes & Nowakowski, 2002). We therefore calculated that about 1300 newly-generated neurons could be integrated into the mature granule cell layer per day, or about 0.02% of the neuron population found in mature monkeys (see below).

Altogether, these data indicate that the postnatal production of neurons and glial cells in the monkey dentate gyrus peaks within the first 3 months after birth. However, this peak is followed by a sustained, intermediate level of neuronal and glial production from 3 months to at least 1 year of age. Thereafter, neurogenesis and gliogenesis persist at a lower, but significant rate in the mature monkey dentate gyrus.

TUNEL staining

Cell death was measured using the TUNEL method. As compared with the number of Ki-67- and BrdU-positive cells, it appears that the sensitivity of our TUNEL assay was not sufficient to detect all dying cells (see data on Neuron number below). Nevertheless, the number of TUNEL-positive cells differed between age groups in the combined

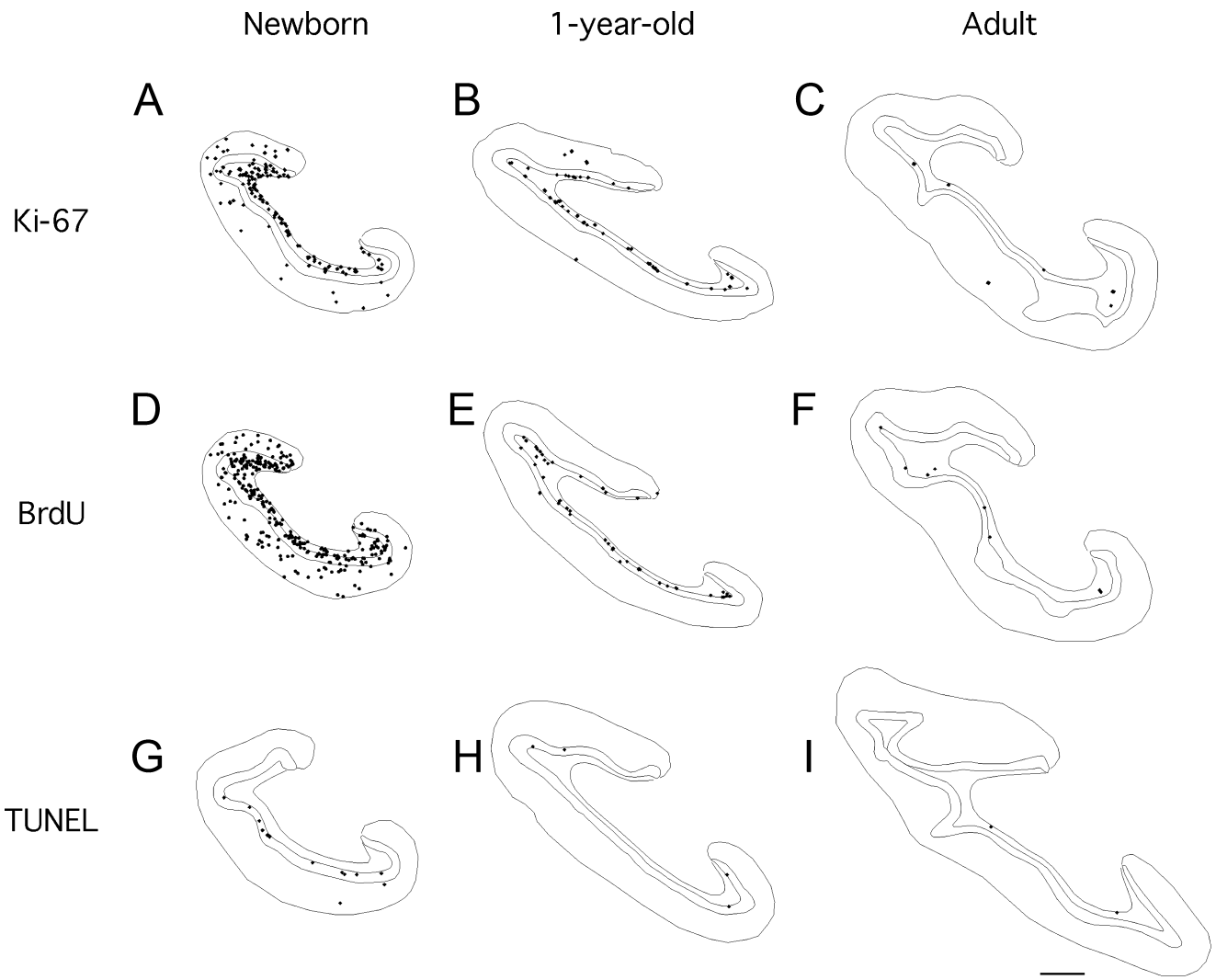

FIG. 4. Representative coronal sections through the monkey dentate gyrus illustrating the location of Ki-67-positive cells (A–C), 5′-bromo-2-deoxyuridine (BrdU)-positive cells 4 weeks after BrdU injection (D–F) and terminal deoxynucleotidyl transferase-mediated dUTP-biotin nick-end labeling (TUNEL)-positive cells (G–I), at different ages through postnatal life (A, D, G: newborns; B, E, H: 1 year olds; C, F, I: 5–10 year olds). Note the different distribution of Ki-67- and BrdU-labeled cells across the polymorphic and granule cell layers. Note also the location of TUNEL-positive cells across all layers of the dentate gyrus, including the granule cell layer. Scale bar: 500 μm (I, applies to all panels).

granule cell and polymorphic layers (Fig. 5; $H = 17.104$, $P = 0.004$). It decreased substantially from birth (1976 ± 493) to 3 months of age (400 ± 134; $P < 0.05$; 20% of birth level). The number of TUNEL-positive cells remained at an intermediate level between 3 months and 1 year of age (average 284 ± 47), and decreased to 1% of newborn levels at 5–10 years of age (24 ± 15; $P < 0.05$).

The number of TUNEL-positive cells in the molecular layer differed between age groups (Fig. 5; $H = 16.018$, $P = 0.007$). It decreased from birth (536 ± 119) to 3 months of age (240 ± 62; $P < 0.05$; 45% of the newborn level). Although we could not demonstrate a significant difference between age groups after 3 months of age (we found an average of 126 ± 40 TUNEL-positive cells between 3 months and 1 year of age), the number of TUNEL-positive cells found in 5–10-year-old monkeys was only about 9% of the level observed at birth (48 ± 9). Interestingly, the quantification of TUNEL-positive cells revealed a developmental profile similar to that of cell proliferation (Fig. 2). However, there was proportionally more cell death relative to cell proliferation in newborn monkeys as compared with all other ages. These data suggest that the integration of new neurons in the granule cell layer of the monkey dentate gyrus during postnatal development and in adulthood is regulated by the balance between cell proliferation, neurogenesis and cell death. Factors influencing cell proliferation, cell differentiation and cell survival are thus likely to influence neuron production throughout the monkeys' entire postnatal life.

Neuron number

The data presented above on cell proliferation, neurogenesis and cell death suggest that neuron addition during the first year of life might impact total neuron number in the monkey granule cell layer. As expected, the stereological analysis of granule cell number in Nissl-stained sections revealed differences between age groups (Fig. 6A; $F_{5,18} = 7.844$, $P < 0.001$). There was a large increase in neuron number between newborn (4.39 ± 0.21 million cells) and 3-month-old monkeys (6.13 ± 0.36 million cells; $P = 0.003$). This represents an average rate of accretion of about 19300 neurons per day. After 3 months of age, neuron number increased gradually at an average rate of about 3100 granule cells per day to reach 6.99 ± 0.47 million

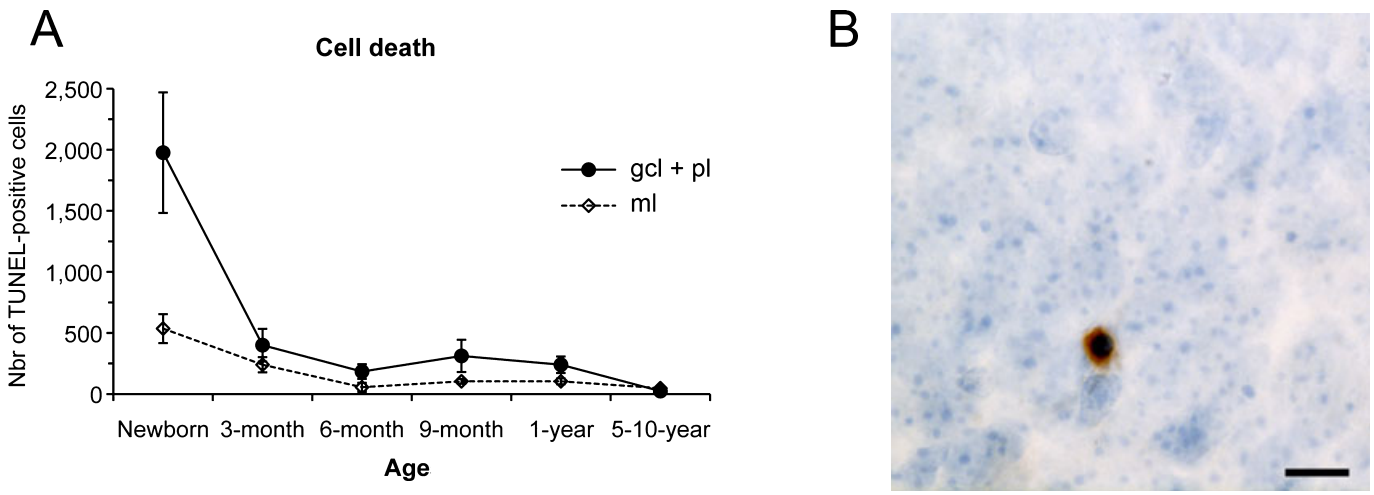

FIG. 5. Terminal deoxynucleotidyl transferase-mediated dUTP-biotin nick-end labeling (TUNEL) staining. (A) Number of TUNEL-positive cells in the molecular layer (white diamonds) and in the combined granule cell and polymorphic layers (black circles) of the macaque monkey dentate gyrus through early postnatal development and in adulthood. (B) Photomicrograph of a TUNEL-positive cell in the granule cell layer. Scale bar: 10 μm. Abbreviations, see Fig. 1.

at 1 year of age. After 1 year of age neuron production and cell death appeared to continue at a lower rate (see above), so that there were about 7.21 ± 0.26 million granule cells in 5–10-year-old monkeys. These numbers, derived from neuron counts with the optical fractionator in Nissl-stained preparations, are very much in line with the results of Ki-67 and BrdU immunohistochemistry described above. Note that these numbers differ somewhat from our preliminary estimates (Amaral & Lavenex, 2007; Lavenex *et al.*, 2007a). We have determined that our preliminary data overestimated the total number of neurons (uniformally across ages) likely due to an error in the calibration of the StereoInvestigator analysis system used previously (Amaral & Lavenex, 2007; Lavenex *et al.*, 2007a). The current estimates are thus more accurate and should be considered for future reference.

Altogether, our findings reveal that about 40% of the total number of neurons found in the granule cell layer of 5–10-year-old monkeys are added postnatally, with a peak during the first 3 months after birth (25%). A stable number of granule cell neurons in 5–10-year-old monkeys, despite a low but substantial level of neurogenesis, suggests a turnover or replacement of granule cell neurons in the mature primate dentate gyrus.

Neuron size

We also measured the volume of neuronal somas in order to further characterize the structural maturation of the granule cell layer throughout postnatal development (Fig. 7). We found a bimodal distribution of cell size across ages (mode 1: < 150 μm^3; mode 2: 400–550 μm^3): a large population of small cells most prominent during the first months after birth gradually gave way to mature cells. Accordingly, the number of small cells differed between age groups ($F_{5,18}$ = 5.183, P = 0.004). After a transient increase in the number of small cells between birth and 3 months of age (P = 0.016), which corresponds to the peak of neurogenesis described above, the small cell population decreased gradually within the first year after birth. Interestingly, the number of small cells was still significantly higher in 1-year-old monkeys as compared with 5–10-year-old monkeys (P = 0.023). Similarly, the number of mature-sized cells differed between age groups ($F_{5,18}$ = 14.582, P < 0.001). The mature-sized cell population exhibited a gradual increase between birth and 1 year of age (newborn < 6 months, 9 months and 1 year, all P < 0.05; 3 months < 1 year, P = 0.005). And, most importantly, the number of mature-sized cells was lower in 1-year-old monkeys, as compared with 5–10 year olds (P = 0.022). These data indicate that monkey granule cell neurons undergo a gradual but substantial structural maturation from birth until beyond the first year after birth in order to achieve mature morphological characteristics.

Developmental profiles of the volumes of the molecular, granule cell and polymorphic layers of the dentate gyrus

The volume of the different layers of the dentate gyrus exhibited distinct developmental profiles. Stereological analysis of the granule cell layer volume in Nissl-stained sections revealed differences between age groups (Fig. 6B; $F_{5,18}$ = 5.718, P = 0.002). At birth, the volume of the granule cell layer (6.43 ± 0.60 mm^3) was about 60% of that observed in 5–10-year-old monkeys (10.77 ± 0.66 mm^3). It increased linearly (0.008 mm^3 per day, R^2 = 0.4667, P < 0.001) between birth and 1 year of age (9.46 ± 0.55 mm^3), when it reached 88% of the volume observed in 5–10-year-old monkeys.

The volume of the molecular layer exhibited a developmental profile similar to that of the granule cell layer (Fig. 6C); it differed significantly between age groups ($F_{5,18}$ = 17.105, P < 0.001). At birth, the volume of the molecular layer (19.97 ± 1.56 mm^3) was 43% of that observed in 5–10-year-old monkeys (46.18 ± 2.54 mm^3). It increased linearly (0.05 mm^3 per day, R^2 = 0.731, P < 0.001) between birth and 1 year of age (39.38 ± 3.21 mm^3), when it reached 85% of the volume observed in 5–10-year-old monkeys.

The volume of the polymorphic layer exhibited a different developmental profile (Fig. 6D). Although the volume of the polymorphic layer also differed between age groups ($F_{5,18}$ = 11.267, P < 0.001), it exhibited only a marginal increase between birth (5.46 ± 0.60 mm^3; 56% of 5–10-year-old size) and 9 months of age (6.57 ± 0.30 mm^3; 67% of 5–10-year-old size). In contrast, it exhibited a significant growth past 9 months and 1 year of age (7.75 ± 0.40 mm^3; 80% of 5–10-year-old size) to reach the volume observed at 5–10 years of age (9.74 ± 0.88 mm^3). The developmental growth pattern of the polymorphic layer within the first postnatal year

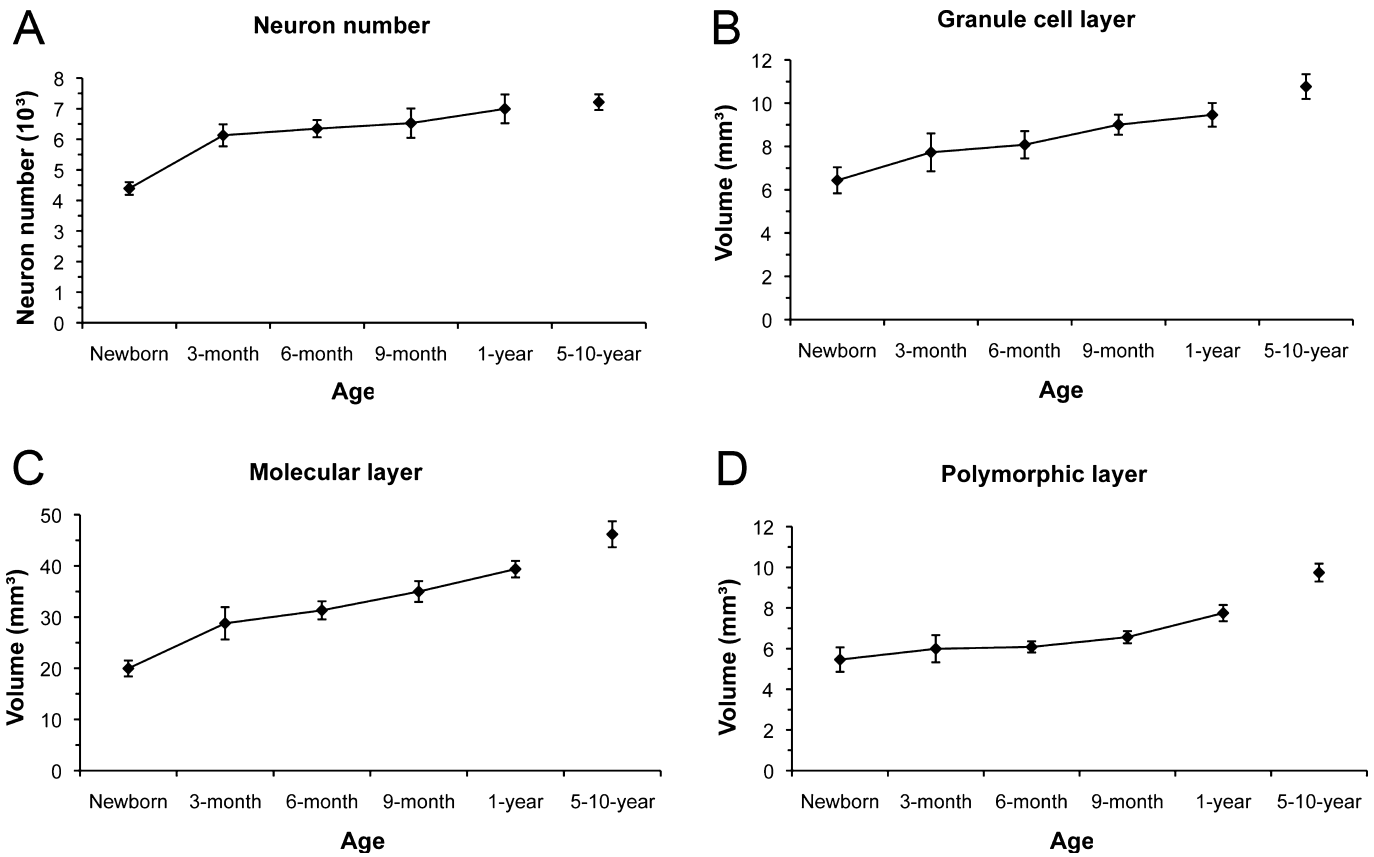

FIG. 6. Total number of neurons in the granule cell layer (A) and volumes (B–D) of the different layers of the macaque monkey dentate gyrus through early postnatal development and in adulthood. Note the large increase in neuron number between birth and 3 months of age, and the gradual increase of about 3100 neurons per day between 3 months and 1 year of age. (B) Volume of the granule cell layer. (C) Volume of the molecular layer. (D) Volume of the polymorphic layer. Note the linear increase in volume of the granule cell and molecular layers between birth and 1 year of age. In contrast, the polymorphic layer exhibits a significant increase only past 9 months and 1 year of age.

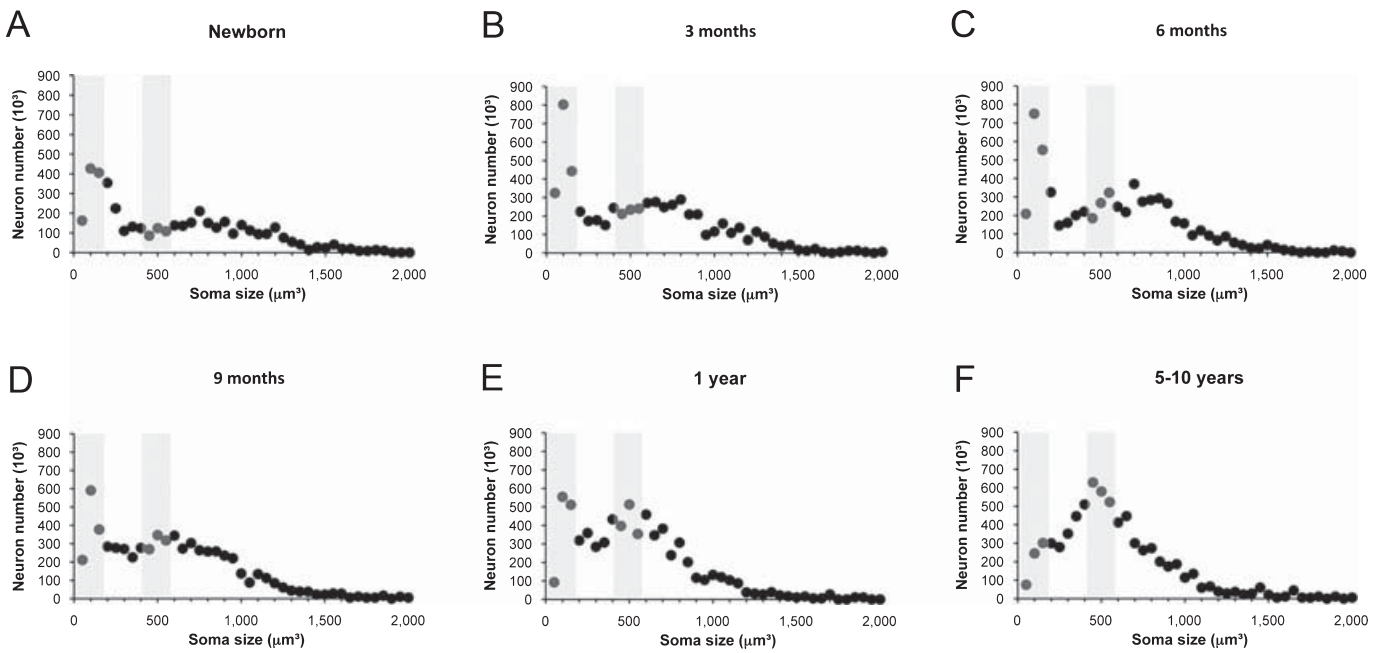

FIG. 7. Bimodal distribution of neuronal soma size in the monkey granule cell layer through early postnatal development and in adulthood. Gray areas indicate the two modes: mode 1, corresponding to immature granule cells (soma < 150 μm^3); mode 2, corresponding to the median size of mature granule cells (400–550 μm^3). (A) newborns; (B) 3-month-olds; (C) 6-month-olds; (D) 9-month-olds; (E) 1-year-olds; (F) 5–10-year-olds.

was not linear, but was best modeled by a polynomial regression ($1E-0.5x^2 + 0.0004x + 5.5734$; $R^2 = 0.4532$, $P = 0.017$).

Summary of results

The aim of this study was to characterize and quantify the fundamental morphological changes underlying the structural maturation of the rhesus macaque monkey (*Macaca mulatta*) dentate gyrus during early postnatal development. Our results demonstrate that the macaque monkey dentate gyrus is far from mature at birth and that about 40% of the total number of granule cells found in 5–10-year-old monkeys are added to the granule cell layer postnatally, with a peak (about 25%) in the first 3 months after birth. These neurons undergo a significant increase in size from birth to beyond 1 year of age in order to achieve mature morphological characteristics. Moreover, the three layers of the dentate gyrus exhibit distinct developmental profiles in their volumetric expansion. Finally, we observe significant levels of cell proliferation, neurogenesis and cell death in the context of an overall stable number of granule cells in mature monkeys.

Discussion

Neurogenesis during early postnatal development and in adulthood

Our findings that about 40% of neurons are added to the monkey granule cell layer after birth are consistent with previous estimates by Seress, who reported 2.8 million granule cells in newborns (Seress, 1992) and 4.8 million in 5–10-year-old macaque monkeys (Seress, 1988). A comparison of his estimates for adult rats (CFY: 892 000; Long-Evans: 656 000; Seress, 1988) with those of others (Long-Evans: 1.2 million, Rapp & Gallagher, 1996; Wistar: 1.2 million, West *et al.*, 1991), as well as his estimates for adult humans (8.81 million, Seress, 1988) with those of others (13 million, Sa *et al.*, 2000; 15 million, West & Gundersen, 1990), indicates that Seress' reports were consistently underestimating neuron number by a factor of about 1.5. Accordingly, our estimates of 4.39 million granule cells in newborns and 7.21 million in adult monkeys are also about 1.5 times those reported previously by Seress (1988, 1992). Unfortunately, there are no reliable data regarding granule cell number in newborn and developing individuals of other species to draw parallels between the developmental profiles of the dentate gyrus across phylogeny.

The developmental period during which a significant number of neurons are added to the monkey granule cell layer is much longer than previously thought. In a preliminary study, we failed to demonstrate differences in neuron number between 3-month-old ($n = 2$) and adult ($n = 6$) macaque monkeys (Lavenex *et al.*, 2007a). Rakic and colleagues also suggested that major neuron production ceases at about 3 months of age (Rakic & Nowakowski, 1981; Eckenhoff & Rakic, 1988). Although we observed a significant decrease in the rate of neuron addition at about 3 months of age in the current study, we calculated that about 3100 neurons are added to the granule cell layer each day between 3 months and 1 year of age. These data, which are derived from stereological counts of neurons in Nissl-stained preparations, are supported by our immunohistochemical findings on cell proliferation, neurogenesis and cell death. Indeed, the number of Ki-67-labeled cells decreased strongly between birth and 3 months of age but remained at an intermediate level, which was 10 times higher than that observed in mature monkeys, between 6 months and 1 year of age. The overall distribution of Ki-67-labeled cells that we described in newborn monkeys was similar to that observed in newborn humans (Seress, 2001). In humans, cell proliferation also seems to persist at least until the end of the first year after birth (the latest age examined immunohistochemically by Seress *et al.*, 2001). However, in the absence of strict quantification of human cases, it is difficult to draw direct parallels between our findings and the human data. Interestingly, neurogenesis evaluated by BrdU/NeuN immunohistochemistry revealed the same developmental profile as Ki-67. We found an intermediate level of neurogenesis between 3 months and 1 year of age (as compared with birth and adulthood), which correlated with the gradual increase in neuron number measured in Nissl-stained preparations.

In agreement with previous studies in adult primates (Eriksson *et al.*, 1998; Gould *et al.*, 1999b; Kornack & Rakic, 1999), we found a persistent level of neurogenesis in mature monkeys. We estimated the number of new neurons that could potentially be integrated in the granule cell layer to be about 1300 per day or 0.02% of the total number of granule cells in mature monkeys. However, this substantial number of newly-generated neurons did not impact total granule cell number in adult individuals. There was no trend towards an increase in neuron number between the youngest and oldest mature monkeys used in our study, suggesting that a number of mature neurons approximately equal to the number of newly-generated granule cells must die and be replaced. Our data are therefore consistent with the results of modern stereological studies showing that the total number of granule cells does not vary in rats between six and 27 months of age (Rapp & Gallagher, 1996) or in C57BL/6J mice between 2 and 9 months of age (Ben Abdallah *et al.*, 2008; see also Kempermann *et al.*, 1998; for C57BL/6N mice between 6 and 18 months of age), despite significant levels of neurogenesis at older ages. A low but significant number of TUNEL-positive cells in the dentate gyrus supports this finding. The location of dying cells in our preparations, in the polymorphic and granule cell layers, is in agreement with other primate and rodent studies (Cameron *et al.*, 1993; Seress, 2001). Altogether these data suggest that some mature neurons must die and be replaced by newly-generated neurons in adulthood to maintain a stable number of dentate granule cells.

In sum, the potential structural impact of postnatal neurogenesis differs in developing and mature individuals. Neurogenesis occurs at a relatively high rate within the monkeys' first postnatal year, impacting the number of granule cells and therefore dentate gyrus structure. Neurogenesis continues at a relatively low rate in adulthood and is therefore unlikely to have a major impact on the fundamental structural organization of the granule cell layer in mature individuals. Our data are consistent with the hypothesis that adult neurogenesis functions as a replacement mechanism in mature individuals (Kirn & Nottebohm, 1993; Banta Lavenex *et al.*, 2001; Kuhn *et al.*, 2001). This idea is also consistent with a recent study showing that the recruitment of new neurons into the adult avian song nucleus HVC is tightly linked to neuronal death (Thompson & Brenowitz, 2009).

Functional implications

Developmental neurogenesis

Defining the critical periods during which particular developmental processes occur is essential to making predictions regarding pathologies that might arise at various stages during development (Prather *et al.*, 2001; Lavenex *et al.*, 2004, 2007b, 2009b). For example, postnatal neurogenesis is reduced in mice reared in deprived conditions between 21 and 61 days of age, leading to a smaller dentate gyrus with fewer granule cells and spatial learning impairments as compared with mice reared in 'enriched' laboratory

conditions (Kempermann *et al.*, 1997). When the same living conditions are imposed on 6- or 18-month-old mice, neurogenesis is also regulated but neither structural nor functional deficits are observed (i.e. no differences in neuron number or swim path lengths in the Morris search task; Kempermann *et al.*, 1998). Similarly, nutritional deficits during the first 2 months affect hippocampal structure and spatial memory later in life in scrub jays (Pravosudov *et al.*, 2005). Most significantly, nutritional rehabilitation from 2 months to 1 year of age does not alleviate the deleterious effects of early malnutrition, suggesting that a critical neurodevelopmental period had passed.

Importantly, MRI evidence of abnormal development of the dentate gyrus (Saitoh *et al.*, 2001) and the hippocampal formation (Schumann *et al.*, 2004) in children with autism has been reported. In monkeys, we can predict that although detrimental or compensatory factors will have the biggest impact on neuron addition during the first 3 months after birth, there is an extended developmental period, from 3 months to at least 1 year of age, during which neuron addition remains sufficiently high to impact neuron number. Compensatory measures applied during this developmental period could serve to alleviate the consequences of early deprivation on granule cell number. In contrast, negative factors (such as environmental or food deprivation) during this period could also impact neuron number and hippocampal function later in life. Rehabilitation past this critical developmental period would likely not compensate for early deprivations. One caveat that arises from these findings is the importance that must be placed on choosing appropriately aged experimental animals when attempting to model human neurodevelopmental disorders (see also McCutcheon & Marinelli, 2009). At this point, however, there is insufficient information to draw strict parallels and define critical neurodevelopmental periods in both humans and animals, which could help translational researchers to develop clinical treatments to alleviate anatomical abnormalities leading to human neurological disorders.

Adult neurogenesis

We estimated the number of new neurons that could potentially be integrated into the granule cell layer of mature monkeys to be about 1300 per day or 0.02% of total neuron number (7.21 million). This rate of adult neurogenesis might appear low as compared with the postnatal neurogenesis reported in rodents. Indeed, Cameron & McKay (2001) estimated that about 2250 new neurons are generated each day in 9–10-week-old rats (unilaterally), which corresponds to about 0.2% of total neuron number (1.2 million). However, considering that monkeys live 20–30 years and rats 2–3 years (Havenaar *et al.*, 1993), postnatal neurogenesis has a similar potential in rodents and primates: that is the renewal of the entire population of granule cells during an individual's lifetime.

The actual number of mature granule cells that might be replaced by newly-generated neurons born in adulthood is difficult to determine with current techniques. Indeed the majority of cells produced during postnatal development die within the first 4 weeks after their birth. However, a significant number of BrdU-labeled cells remain after 4 weeks and this number appears stable for at least 11 months in mice (Kempermann *et al.*, 2003), suggesting that the investigation of neurogenesis 4 weeks after the injection of the proliferation marker BrdU allows a good estimate of the long-term survival and potential structural impact of newly-generated neurons. Consistent with previous data in rodents (Cameron *et al.*, 1993; Cameron & McKay, 2001; Kempermann *et al.*, 2003), our current results suggest that new cells are generated in surplus and constitute a pool of immature neurons that can potentially be recruited into functional circuits (Toni *et al.*, 2008). Interestingly, in 2-month-old C57BL/6N mice about 40% of these newly-generated cells migrate into the outer two-thirds of the granule cell layer within 4 weeks (Kempermann *et al.*, 2003). In our study, 88% of the BrdU/NeuN-labeled cells present 4 weeks after BrdU injection in 5–10-year-old monkeys were located in the granule cell layer. Altogether, these data indicate that a significant number of newly-generated neurons are integrated in the granule cell layer of mature individuals without impacting the total number of neurons in this structure.

Recent computational models of the role of neurogenesis in hippocampal function hypothesized that the adult-generated neurons are added to the population of mature granule cells, leading to a gradual increase in the total number of neurons (Aimone *et al.*, 2009; Weisz & Argibay, 2009). Our current results, together with those of previous studies in rodents (Rapp & Gallagher, 1996; Kempermann *et al.*, 1998; Ben Abdallah *et al.*, 2008), demonstrate that this assumption is invalid for mature individuals (that is, past a certain postnatal developmental period that extends for several weeks in rodents and several months in primates). Nevertheless, both models make the interesting prediction that newly-generated immature neurons might contribute to increased association of events occurring close in time, whereas events occurring several days apart would be encoded separately by distinct groups of newly-generated neurons that are not yet fully mature (Aimone *et al.*, 2009; Weisz & Argibay, 2009). In conjunction with the reported role of the dentate gyrus in pattern separation (Clelland *et al.*, 2009), adult neurogenesis could help to disambiguate new events happening in familiar contexts and therefore contribute to the encoding of individual episodic memories (Aimone *et al.*, 2009). What should be considered in future models, however, is the impact of neuron replacement (as the total number of granule cells does not vary in mature individuals, some neurons must die and be replaced) on the long-term maintenance and retrieval of memories in hippocampal circuits.

Conclusion

Our quantitative analyses provide critical information regarding the relative importance of postnatal neurogenesis and its impact on neuron number in the primate dentate gyrus. First, we identified an extended developmental period during which neurogenesis leads to increased neuron number in the monkey dentate gyrus. Postnatal neurogenesis occurring during this developmental period must therefore be clearly distinguished from adult neurogenesis that occurs in mature animals. Second, the relative importance of adult neurogenesis might be similar in rodents and primates, if we consider the lifespan in each species. Specifically, our data suggest that the combination of cell death and neurogenesis have the potential to renew the entire population of granule cells across an individual's lifespan in both rodents and primates.

Supporting Information

Additional supporting information may be found in the online version of this article:

Table S1. Total number of BrdU-labeled cells expressing a neuronal marker (NeuN), a glial marker (S100beta) or neither, in the combined granule cell and polymorphic layers of the dentate gyrus in macaque monkeys (*Macaca mulatta*) through early postnatal development and in adulthood. Monkeys received an i.p. injection of BrdU (150 mg/kg) 4 weeks prior to brain collection.

Table S2. Total number of BrdU-labeled cells expressing a neuronal marker (NeuN), a glial marker (S100beta) or neither, in the molecular layer of the dentate gyrus in macaque monkeys (*Macaca mulatta*) through early postnatal development and in adulthood. Monkeys received an i.p. injection of BrdU (150 mg/kg) 4 weeks prior to brain collection.

Please note: As a service to our authors and readers, this journal provides supporting information supplied by the authors. Such materials are peer-reviewed and may be re-organized for online delivery, but are not copy-edited or typeset by Wiley-Blackwell. Technical support issues arising from supporting information (other than missing files) should be addressed to the authors.

Acknowledgements

This research was supported by NIH grant (RO1-NS16980), Swiss National Science Foundation grants (PP00A-106701, PP00P3-124536) and was conducted, in part, at the California National Primate Research Center (RR00169). We thank the CNPRC staff, Jeff Bennett, K.C. Brown, Loïc Chareyron, Grégoire Favre, Jane Favre and Danièle Uldry for technical assistance at various stages of the project.

Abbreviations

BrdU, 5′-bromo-2-deoxyuridine; DAB, diaminobenzidine; NDS, normal donkey serum; NGS, normal goat serum; PB, phosphate buffer; PBS, phosphate-buffered saline; TCS, tissue collection solution; TUNEL, terminal deoxynucleotidyl transferase-mediated dUTP-biotin nick-end labeling; TX-100, Triton X-100.

References

Aimone, J.B., Wiles, J. & Gage, F.H. (2009) Computational influence of adult neurogenesis on memory encoding. *Neuron*, **61**, 187–202.

Altemus, K.L., Lavenex, P., Ishizuka, N. & Amaral, D.G. (2005) Morphological characteristics and electrophysiological properties of CA1 pyramidal neurons in macaque monkeys. *Neuroscience*, **136**, 741–756.

Altman, J. & Das, G.D. (1965) Autoradiographic and histological evidence of postnatal hippocampal neurogenesis in rats. *J. Comp. Neurol.*, **124**, 319–335.

Amaral, D.G. & Lavenex, P. (2007) Hippocampal neuroanatomy. In Amaral, D.G., Andersen, P., Bliss, T., Morris, R.G.M. & O'Keefe, J. (Eds), *The Hippocampus Book*. Oxford University Press, New York, pp. 37–114.

Amaral, D.G., Scharfman, H.E. & Lavenex, P. (2007) The dentate gyrus: fundamental neuroanatomical organization (dentate gyrus for dummies). *Prog. Brain Res.*, **163**, 3–22.

Amrein, I., Slomianka, L. & Lipp, H.P. (2004) Granule cell number, cell death and cell proliferation in the dentate gyrus of wild-living rodents. *Eur. J. Neurosci.*, **20**, 3342–3350.

Arnold, S.E. & Trojanowski, J.Q. (1996) Human fetal hippocampal development. 1. Cytoarchitecture, myeloarchitecture, and neuronal morphologic features. *J. Comp. Neurol.*, **367**, 274–292.

Banta Lavenex, P., Lavenex, P. & Clayton, N.S. (2001) Comparative studies of postnatal neurogenesis and learning: a critical review. *Av. Poult. Biol. Rev.*, **12**, 103–125.

Banta Lavenex, P., Amaral, D.G. & Lavenex, P. (2006) Hippocampal lesion prevents spatial relational learning in adult macaque monkeys. *J. Neurosci.*, **26**, 4546–4558.

Ben Abdallah, N.M.-B., Slomianka, L., Vyssotski, A.L. & Lipp, H.-P. (2008) Early age-related changes in adult hippocampal neurogenesis in C57 mice. *Neurobiol. Aging*, DOI: 10.1016/j.neurobiolaging.2008.03.002.

Biebl, M., Cooper, C.M., Winkler, J. & Kuhn, H.G. (2000) Analysis of neurogenesis and programmed cell death reveals a self-renewing capacity in the adult rat brain. *Neurosci. Lett.*, **291**, 17–20.

Cameron, H.A. & McKay, R.D. (2001) Adult neurogenesis produces a large pool of new granule cells in the dentate gyrus. *J. Comp. Neurol.*, **435**, 406–417.

Cameron, H.A., Woolley, C.S., McEwen, B.S. & Gould, E. (1993) Differentiation of newly born neurons and glia in the dentate gyrus of the adult rat. *Neuroscience*, **56**, 337–344.

Clelland, C.D., Choi, M., Romberg, C., Clemenson, G.D. Jr, Fragniere, A., Tyers, P., Jessberger, S., Saksida, L.M., Barker, R.A., Gage, F.H. & Bussey, T.J. (2009) A functional role for adult hippocampal neurogenesis in spatial pattern separation. *Science*, **325**, 210–213.

Courchesne, E. (2002) Abnormal early brain development in autism. *Mol. Psychiatry*, **7**, S21–S23.

Eckenhoff, M.F. & Rakic, P. (1984) Radial organization of the hippocampal dentate gyrus a Golgi ultrastructural and immuno cytochemical analysis in the developing rhesus monkey *Macaca-mulatta*. *J. Comp. Neurol.*, **223**, 1–21.

Eckenhoff, M.F. & Rakic, P. (1988) Nature and fate of proliferative cells in the hippocampal dentate gyrus during the life span of the rhesus monkey. *J. Neurosci.*, **8**, 2729–2747.

Eriksson, P.S., Perfilieva, E., Bjork-Eriksson, T., Alborn, A.-M., Nordborg, C., Peterson, D.A. & Gage, F.H. (1998) Neurogenesis in the adult human hippocampus. *Nat. Med.*, **4**, 1313–1317.

Gavrieli, Y., Sherman, Y. & Ben-Sasson, S.A. (1992) Identification of programmed cell death in situ via specific labeling of nuclear DNA fragmentation. *J. Cell Biol.*, **119**, 493–501.

Giedd, J.N., Vaituzis, A.C., Hamburger, S.D., Lange, N., Rajapakse, J.C., Kaysen, D., Vauss, Y.C. & Rapoport, J.L. (1996) Quantitative MRI of the temporal lobe, amygdala, and hippocampus in normal human development: ages 4-18 years. *J. Comp. Neurol.*, **366**, 223–230.

Gould, E. & Gross, C.G. (2002) Neurogenesis in adult mammals: some progress and problems. *J. Neurosci.*, **22**, 619–623.

Gould, E., Tanapat, P., McEwen, B.S., Flugge, G. & Fuchs, E. (1998) Proliferation of granule cell precursors in the dentate gyrus of adult monkeys in diminished by stress. *Proc. Natl Acad. Sci. USA*, **95**, 3168–3171.

Gould, E., Tanapat, P., Hastings, N.B. & Shors, T.J. (1999a) Neurogenesis in adulthood: a possible role in learning. *Trends Cogn. Sci.*, **3**, 186–192.

Gould, E., Reeves, A.J., Fallah, M., Tanapat, P., Gross, C.G. & Fuchs, E. (1999b) Hippocampal neurogenesis in adult Old World primates. *Proc. Natl Acad. Sci. USA*, **96**, 5263–5267.

Gundersen, H.J. (1988) The nucleator. *J. Microsc.*, **151**, 3–21.

Gundersen, H.J. & Jensen, E.B. (1987) The efficiency of systematic sampling in stereology and its prediction. *J. Microsc.*, **147**, 229–263.

Harrison, P.J. (1999) The neuropathology of schizophrenia. A critical review of the data and their interpretation. *Brain*, **122**, 593–624.

Havenaar, R., Meijer, J.C., Morton, D.B., Ritskes-Hoitinga, J. & Zwart, P. (1993) Biology and husbandry of laboratory animals. In Van Zutphen, L.F.M., Baumans, V. & Beynen, A.C. (Eds), *Principles of Laboratory Animal Science*. Elsevier Science, Netherlands, pp. 17–74.

Hayes, N.L. & Nowakowski, R.S. (2002) Dynamics of cell proliferation in the adult dentate gyrus of two inbred strains of mice. *Brain Res. Dev. Brain Res.*, **134**, 77–85.

Kempermann, G. (2002) Why new neurons? Possible functions for adult hippocampal neurogenesis. *J. Neurosci.*, **22**, 635–638.

Kempermann, G., Kuhn, H.G. & Gage, F.H. (1997) More hippocampal neurons in adult mice living in an enriched environment. *Nature*, **386**, 493–495.

Kempermann, G., Kuhn, H.G. & Gage, F.H. (1998) Experienced-induced neurogenesis in the senescent dentate gyrus. *J. Neurosci.*, **18**, 3206–3212.

Kempermann, G., Gast, D., Kronenberg, G., Yamaguchi, M. & Gage, F.H. (2003) Early determination and long-term persistence of adult-generated new neurons in the hippocampus of mice. *Development*, **130**, 391–399.

Kirn, J.R. & Nottebohm, F. (1993) Direct evidence for loss and replacement of projection neurons in adult canary brain. *J. Neurosci.*, **13**, 1654–1663.

Kolb, B., Pedersen, B., Ballermann, M., Gibb, R. & Whishaw, I.Q. (1999) Embryonic and postnatal injections of bromodeoxyuridine produce age-dependent morphological and behavioral abnormalities. *J. Neurosci.*, **19**, 2337–2346.

Kornack, D.R. & Rakic, P. (1999) Continuation of neurogenesis in the hippocampus of the adult macaque monkey. *Proc. Natl Acad. Sci. USA*, **96**, 5768–5773.

Kuhn, H.G., Palmer, T.D. & Fuchs, E. (2001) Adult neurogenesis: a compensatory mechanism for neuronal damage. *Eur. Arch. Psychiatry Clin. Neurosci.*, **251**, 152–158.

Lavenex, P. (2009) Neuroanatomy methods in humans and animals. In Squire, L.R. (Ed.), *Encyclopedia of Neuroscience*. Academic Press, Oxford, pp. 269–278.

Lavenex, P. & Amaral, D.G. (2000) Hippocampal-necortical interaction: a hierarchy of associativity. *Hippocampus*, **10**, 420–430.

Lavenex, P., Steele, M.A. & Jacobs, L.F. (2000a) The seasonal pattern of cell proliferation and neuron number in the dentate gyrus of wild adult eastern grey squirrels. *Eur. J. Neurosci.*, **12**, 1–6.

Lavenex, P., Steele, M.A. & Jacobs, L.F. (2000b) Sex differences, but no seasonal variations in the hippocampus of food-caching squirrels: a stereological study. *J. Comp. Neurol.*, **425**, 152–166.
Lavenex, P., Banta Lavenex, P. & Amaral, D.G. (2004) Nonphosphorylated high-molecular-weight neurofilament expression suggests early maturation of the monkey subiculum. *Hippocampus*, **14**, 797–801.
Lavenex, P., Banta Lavenex, P. & Amaral, D.G. (2007a) Postnatal development of the primate hippocampal formation. *Dev. Neurosci.*, **29**, 179–192.
Lavenex, P., Banta Lavenex, P. & Amaral, D.G. (2007b) Spatial relational learning persists following neonatal hippocampal lesions in macaque monkeys. *Nat. Neurosci.*, **10**, 234–239.
Lavenex, P., Banta Lavenex, P., Bennett, J.L. & Amaral, D.G. (2009a) Postmortem changes in the neuroanatomical characteristics of the primate brain: hippocampal formation. *J. Comp. Neurol.*, **512**, 27–51.
Lavenex, P., Sugden, S.G., Davis, R.R., Gregg, J.P. & Banta Lavenex, P. (2009b) Developmental regulation of gene expression and astrocytic processes may explain selective hippocampal vulnerability. *Hippocampus*, in press. [DOI: 10.1002/hipo.20730].
McCutcheon, J.E. & Marinelli, M. (2009) Age matters. *Eur. J. Neurosci.*, **29**, 997–1014.
Namba, T., Mochizuki, H., Onodera, M., Mizuno, Y., Namiki, H. & Seki, T. (2005) The fate of neural progenitor cells expressing astrocytic and radial glial markers in the postnatal dentate gyrus. *Eur. J. Neurosci.*, **22**, 1928–1941.
Nottebohm, F. (2002) Why are some neurons replaced in adult brain? *J. Neurosci.*, **22**, 624–628.
Nowakowski, R.S. & Rakic, P. (1981) The site of origin and route and rate of migration of neurons to the hippocampal region of the rhesus monkey. *J. Comp. Neurol.*, **196**, 126–154.
Oppenheim, R.W., Flavell, R.A., Vinsant, S., Prevette, D., Kuan, C.Y. & Rakic, P. (2001) Programmed cell death of developing mammalian neurons after genetic deletion of caspases. *J. Neurosci.*, **21**, 4752–4760.
Prather, M.D., Lavenex, P., Mauldin-Jourdain, M.L., Mason, W.A., Capitanio, J.P., Mendoza, S.P. & Amaral, D.G. (2001) Increased social fear and decreased fear of objects in monkeys with neonatal amygdala lesions. *Neuroscience*, **106**, 653–658.
Pravosudov, V.V., Lavenex, P. & Clayton, N.S. (2002) Changes in spatial memory mediated by experimental variation in food supply do not affect hippocampal anatomy in mountain chickadees (*Poecile gambeli*). *J. Neurobiol.*, **51**, 142–148.
Pravosudov, V.V., Lavenex, P. & Omanska, A. (2005) Nutritional deficits during early development affect hippocampal structure and spatial memory later in life. *Behav. Neurosci.*, **119**, 1368–1374.
Rakic, P. (1985) Limits of neurogenesis in primates. *Science*, **227**, 1054–1056.
Rakic, P. & Nowakowski, R.S. (1981) The time of origin of neurons in the hippocampal region of the rhesus monkey. *J. Comp. Neurol.*, **196**, 99–128.
Rapp, P.R. & Gallagher, M. (1996) Preserved neuron number in the hippocampus of aged rats with spatial learning deficits. *Proc. Natl Acad. Sci. USA*, **93**, 9926–9930.
Sa, M.J., Madeira, M.D., Ruela, C., Volk, B., Mota-Miranda, A., Lecour, H., Gonçalves, V. & Paula-Barbosa, M.M. (2000) AIDS does not alter the total number of neurons in the hippocampal formation but induces cell atrophy: a stereological study. *Acta Neuropathol.*, **99**, 643–653.
Saitoh, O., Karns, C.M. & Courchesne, E. (2001) Development of the hippocampal formation from 2 to 42 years: MRI evidence of smaller area dentata in autism. *Brain*, **124**, 1317–1324.
Schumann, C.M., Hamstra, J., Goodlin-Jones, B.L., Lotspeich, L.J., Kwon, H., Buonocore, M.H., Lammers, C.R., Reiss, A.L. & Amaral, D.G. (2004) The amygdala is enlarged in children but not in adolescents with autism; the hippocampus is enlarged at all ages. *J. Neurosci.*, **24**, 6392–6401.
Seress, L. (1988) Interspecies comparison of the hippocampal formation shows increased emphasis on the regio superior in the Ammon's horn of the human brain. *J. Hirnforsch.*, **29**, 335–340.
Seress, L. (1992) Morphological variability and developmental aspects of monkey and human granule cells: differences between the rodent and primate dentate gyrus. *Epilepsy Res. Suppl.*, **7**, 3–28.
Seress, L. (2001) Morphological changes of the human hippocampal formation from midgestation to early childhood. In Nelson, C.A. & Luciana, M. (Eds), *Handbook of Developmental Cognitive Neuroscience*. The MIT Press, Cambridge, MA, pp. 45–58.
Seress, L., Abraham, H., Tornoczky, T. & Kosztolanyi, G. (2001) Cell formation in the human hippocampal formation from mid-gestation to the late postnatal period. *Neuroscience*, **105**, 831–843.
Sloviter, R.S. (1994) The functional organization of the hippocampal dentate gyrus and its relevance to the pathogenesis of temporal lobe epilepsy. *Ann. Neurol.*, **35**, 640–654.
Thompson, C.K. & Brenowitz, E.A. (2009) Neurogenesis in an adult avian song nucleus is reduced by decreasing caspase-mediated apoptosis. *J. Neurosci.*, **29**, 4586–4591.
Toni, N., Laplagne, D.A., Zhao, C., Lombardi, G., Ribak, C.E., Gage, F.H. & Schinder, A.F. (2008) Neurons born in the adult dentate gyrus form functional synapses with target cells. *Nat. Neurosci.*, **11**, 901–907.
Weisz, V.I. & Argibay, P.F. (2009) A putative role for neurogenesis in neurocomputational terms: inferences from a hippocampal model. *Cognition*, **112**, 229–240.
West, M.J. & Gundersen, H.J.G. (1990) Unbiased stereological estimation of the number of neurons in the human hippocampus. *J. Comp. Neurol.*, **296**, 1–22.
West, M.J., Slomianka, L. & Gundersen, H.J.G. (1991) Unbiased stereological estimation of the total number of neurons in the subdivisions of the rat hippocampus using the optical fractionator. *Anat. Rec.*, **231**, 482–497.